

# On Representation Knowledge Distillation for Graph Neural Networks

Chaitanya K. Joshi, Fayao Liu, Xu Xun, Jie Lin, Chuan Sheng Foo

**Abstract**—Knowledge distillation is a promising learning paradigm for boosting the performance and reliability of resource-efficient graph neural networks (GNNs) using more expressive yet cumbersome teacher models. Past work on distillation for GNNs proposed the Local Structure Preserving loss (LSP), which matches *local* structural relationships across the student and teacher’s node embedding spaces. In this paper, we make two key contributions:

From a methodological perspective, we study whether preserving the *global* topology of how the teacher embeds graph data can be a more effective distillation objective for GNNs, as real-world graphs often contain latent interactions and noisy edges. The purely local LSP objective over pre-defined edges is unable to achieve this as it ignores relationships among disconnected nodes. We propose two new approaches which better preserve global topology: (1) Global Structure Preserving loss (GSP), which extends LSP to incorporate all pairwise interactions; and (2) Graph Contrastive Representation Distillation (G-CRD), which uses contrastive learning to align the student node embeddings to those of the teacher in a shared representation space.

From an experimental perspective, we introduce an expanded set of benchmarks on large-scale real-world datasets where the performance gap between teacher and student GNNs is non-negligible. We believe this is critical for testing the efficacy and robustness of knowledge distillation, but was missing from the LSP study which used synthetic datasets with trivial performance gaps. Experiments across 4 datasets and 14 heterogeneous GNN architectures show that G-CRD consistently boosts the performance and robustness of lightweight GNN models, outperforming the structure preserving approaches, LSP and GSP, as well as baselines adapted from 2D computer vision. An analysis of the representational similarity among teacher and student embedding spaces reveals that G-CRD strikes a balance between preserving both local and global relationships, while LSP/GSP are best at preserving one or the other.

**Index Terms**—Knowledge Distillation, Graph Neural Networks, Geometric Deep Learning, Contrastive Learning.

## I. INTRODUCTION

GRAPH Neural Networks (GNNs) [1]–[5] aim to generalize convolutional networks from 2D computer vision to irregular data structures such as graphs, sets, and 3D point clouds. Recent years have seen impactful real-world applications of GNNs in fields ranging from social networks [6], [7] to biomedical discovery [8]–[10]. While the community has recently focused on large-scale datasets [11]–[13], more expressive architectures [14]–[17] as well as improving generalization via self-supervised learning [18]–[21], there has been an emerging line of work on lightweight, resource-efficient GNNs [22]–[28] that achieve high performance under computation and

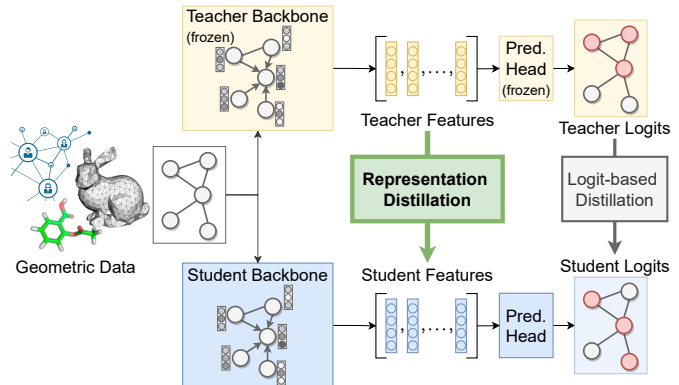


Fig. 1: Knowledge distillation pipeline for graph neural networks. Logit-based distillation transfers dark knowledge about the data domain via matching the logits of the lightweight student to those of the cumbersome teacher. In this work, we investigate *representation distillation*, which transfers representational knowledge using the teacher and student embedding spaces, instead.

memory constraints. Boosting the performance and reliability of such lightweight models is critical for accelerating a myriad of applications, including real-time recommendations on social networks, safety-critical 3D perception for autonomous robots, and encrypted models for proprietary biomedical data.

One promising generic approach for improving the performance of lightweight deep learning models is Knowledge Distillation (KD) [29]. KD is a teacher-student learning paradigm that transfers knowledge from high performance but resource-intensive teacher models to resource-efficient students, see Fig.1. Pioneered by Hinton et al. [29], *logit-based* distillation trains the student to match the output logits of teacher models in addition to standard supervised learning. Recent work has attempted to go beyond logit-based distillation by transferring *representational* knowledge from the teacher to the student through the design of loss functions that align the latent embedding spaces of the teacher and student [30], see Fig.2(a) for an intuitive overview.

Unlike for 2D image data, representation distillation for GNNs has largely been unexplored. To the best of our knowledge, the only representation distillation method for GNNs is the pioneering work of Yang et al. [31] that proposes a **Local Structure Preserving** (LSP) loss to encourage the student to mimic the pairwise similarities with immediate neighbours present in the teacher’s node embedding space, see Fig.2(b). However, preserving only the local pairwise similarities is not guaranteed to preserve the global topology of how the teacher embeds graphs, as this ignores latent interactions among

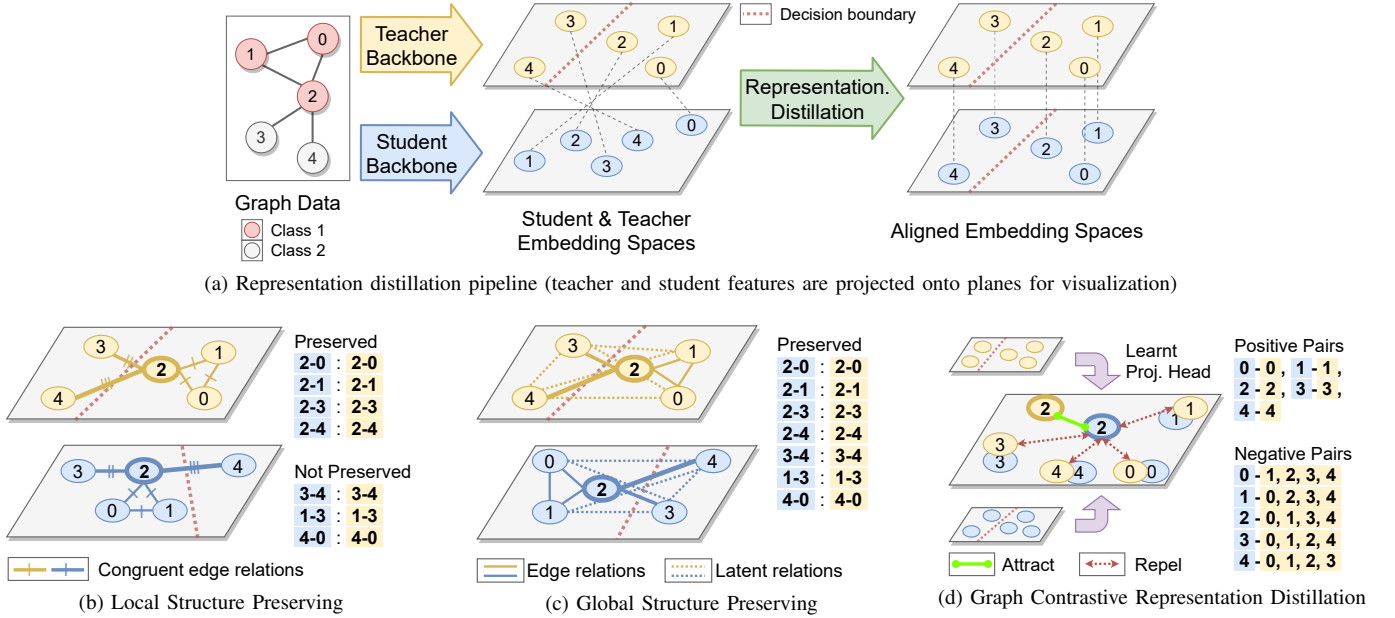


Fig. 2: **Representation distillation for graph neural networks.** (a) Representational knowledge is transferred by aligning the latent node embedding space of the student to that of the teacher. (b) **Local Structure Preserving** loss [31] considers pairwise relationships over graph edges, but may not preserve global topology of the teacher’s embedding space due to latent interactions among disconnected nodes. (c) Preserving all pairwise relationships, *i.e.* **Global Structure Preserving** loss, better preserves the global topology of the embedding space, but can be challenging to optimize/scale up due to an explosion of possible pairs. (d) Different from relation-based approaches, **Graph Contrastive Representation Distillation** transfers representational knowledge by contrastive learning among positive/negative pairwise relations *across* the teacher and student embedding spaces via learnt projection heads.

disconnected nodes. This is often critical for real-world graphs, which tend to be incomplete or noisy as edges are determined heuristically or experimentally. Thus, we explore if preserving global structure can improve representation distillation.

To preserve global relationships, we firstly extend LSP to *explicitly* consider all possible pairwise similarities among node features. However, we found this **Global Structure Preserving** (GSP) approach to be challenging to scale as the number of possible relationships may explode, see Fig.2(c).

An alternative approach is to directly align the node feature vectors, which would *implicitly* preserve all possible relationships as an objective on the features would be a stronger constraint than GSP. To do so, we can regress the student vectors on to the teacher via projection heads [32]–[34] or attention maps [35]. Such ‘feature mimicking’ approaches have been successful for 2D vision, but we and others [31] have observed that they do not boost the performance of student GNNs as there tends to be significant mismatch in representational capacity between expressive teacher architectures and lightweight models in real-world scenarios [36].

Thus, we introduce a new distillation objective that implicitly preserves global topology by aligning the student and teacher node feature vectors in a shared representation space via contrastive learning [37]–[39]. We formulate our objective as a node-level contrastive task on pairwise relationships *across* the teacher and student embedding spaces, see Fig.2(d). We maximize a similarity metric among pairs of corresponding student and teacher node features (similar to mimicking), while additionally minimizing the similarity among pairs of unmatched nodes. We term this objective **Graph Contrastive**

**Representation Distillation (G-CRD)**, as it generalizes CRD [40] from sample-level 2D image classification tasks to fine-grained node-level tasks on graphs.

We compare GSP and G-CRD to baseline distillation techniques and LSP across a diverse range of model architectures and tasks from the popular Open Graph Benchmarks [11] and S3DIS [41]. Crucially, our evaluation focuses on out-of-distribution generalization on real-world data, where the performance gap between cumbersome teachers and lightweight students is non-negligible. We believe this is critical for testing the efficacy and robustness of knowledge distillation, but was missing from the LSP study [31] which used small-scale and synthetic datasets with negligible performance gaps between teachers and students. In addition to our technical contributions, we hope that our expanded set of benchmarks can form the basis for comparison in future work. **Our contributions are summarized as follows:**

- We study GNN representation distillation from the perspective of preserving global topology. We introduce Graph Contrastive Representation Distillation (G-CRD), the first contrastive distillation technique specialized for GNNs, and Global Structure Preserving loss (GSP), an extension of the Local Structure Preserving loss (LSP) [42].
- We benchmark GNN distillation on large-scale datasets which test out-of-distribution generalization, as we are motivated by real-world and real-time applications. Our experiments compare 6 distillation techniques across 4 tasks and 14 architectures for teachers and students. This extends the LSP study which used synthetic datasets with negligible performance gap between teachers and students.

- Training lightweight GNNs with G-CRD consistently outperform the structure preserving objectives, LSP and GSP, as well as baselines adapted from 2D computer vision. We further analyze the robustness, transferability, quantizability, and representational similarity of teacher and student embeddings in order to unpack the efficacy of G-CRD over the structure preserving approaches.

## II. RELATED WORK

**Graph Neural Networks (GNNs).** GNNs [1]–[5] generalize convolutional networks from 2D computer vision to graph structured data. GNNs serve as powerful feature extractors for real-world and real-time applications across diverse domains, including social networks [6], [7], biomedicine [8]–[10], 3D perception [3], [15], and operations research [43], [44]. Our study complements an emerging line of work on efficient GNNs, including lightweight models [22]–[24], neural architecture search [25], [26] and quantization techniques [27], [28].

**Knowledge Distillation (KD).** KD [29] is a learning paradigm for improving the performance of lightweight ‘student’ models by matching their outputs to those from cumbersome ‘teacher’ models. A vast body of literature has developed around augmenting or replacing Hinton et al.’s [29] logit-based approach with *representational knowledge* from the teacher’s latent feature vectors. Following the taxonomy in [30], *feature-based* distillation techniques train the student to imitate the teacher’s intermediate feature vectors or attention maps via direct regression [32]–[35]. Due to mismatches in representational capacity between the teacher and student, feature-based distillation may not improve the performance of lightweight students. As an alternative, *relation-based* distillation preserves metrics among feature vectors from the teacher’s representation space to that of the student, *e.g.* semantic similarity graphs, pairwise distances or angular relationships among samples from the dataset [45]–[47]. The Local Structure Preserving loss (LSP) [31] and its global variant (GSP) extend relation-based distillation for graph data.

Motivated by the success of contrastive objectives for self-supervised learning [37]–[39], Tian et al. [40] proposed Contrastive Representation Distillation (CRD) for 2D image classification. In this work, we found that the sample-level CRD objective is not effective for distilling node-level representations built by GNNs. We introduce Graph Contrastive Representation Distillation (G-CRD), a node-level contrastive distillation objective tailored to GNNs.

**Knowledge Distillation and GNNs.** Local Structure Preserving loss (LSP) [31] is the only distillation technique specifically designed for GNNs and message passing style models, but was evaluated on small-scale synthetic datasets. This work extends the LSP study in two ways: (1) We benchmark distillation techniques on large-scale real-world datasets which explicitly evaluate for out-of-distribution generalization, as well as across a wider range of heterogeneous teacher-student combinations; and (2) We introduce GSP and G-CRD, two new representation distillation objectives that preserve global topology and consistently outperform LSP.

The original logit-based KD [29] has been applied in the GNN literature to improve the training of lightweight models

such as graph-agnostic MLPs or label propagation for node classification [42], [48], [49]. These works do not introduce new GNN-specific distillation techniques. Data-free or teacher-free self-distillation [50]–[52] has also been used to regularize the training of GNNs in the semi-supervised and self-supervised learning paradigm.

Finally, concurrent works on pre-training GNNs for molecular property prediction have also successfully employed contrastive objectives similar to G-CRD to transfer knowledge about 3D molecular geometry into GNNs [53], [54], but do not focus on model compression.

## III. REPRESENTATION DISTILLATION FOR GNNs

### A. Graph Representation Learning

Graph Neural Networks (GNNs) take as input an unordered set of nodes and the graph connectivity among them, and learn latent node representations for them via iterative feature aggregation or message passing across local neighborhoods [5]. Consider a graph  $\mathcal{G} = (\mathcal{V}, \mathcal{E})$ , where  $\mathcal{V}$  is a set of  $n$  nodes, and  $\mathcal{E}$  is a set of edges associated with the nodes. Each node  $i \in \mathcal{V}$  is associated with a  $d$ -dimensional initial feature vector  $f_i$ , which is iteratively updated by the backbone GNN via a generic message passing or graph convolution operation:

$$f_i^{\ell+1} = \text{UPD} \left( f_i^\ell, \text{AGG}_{(i,j) \in \mathcal{E}} \left( \text{MSG}(f_i^\ell, f_j^\ell, e_{ij}) \right) \right), \quad (1)$$

where MSG, UPD are learnable transformations such as multi-layer perceptrons,  $e_{ij}$  are optional edge features for each pair of linked nodes  $i, j$ , and AGG is a permutation-invariant local neighborhood aggregation function such as summation, maximization, averaging, or weighted averaging via attention.

We are usually interested in making predictions for each node in the graph, *e.g.* node classification on social networks or semantic segmentation of 3D point clouds. Thus, the final feature vectors after  $L$  layers of message passing  $f_i^L$  are passed to a linear classifier to obtain logits  $z_i$ , and the neural network is trained end-to-end via a cross-entropy loss  $\mathcal{H}$  with the groundtruth class labels  $y_i$ :  $\mathcal{L}_{\text{SUP}} = \mathcal{H}(y_i, \text{softmax}(z_i))$ .

For graph-level tasks, such as molecular property prediction, the feature vectors of all nodes are pooled via a permutation-invariant function POOL to obtain a global feature vector  $f_G = \text{POOL}(f_i^L | i \in \mathcal{V})$ , and then passed to a linear classifier. Notably, representation learning still occurs at the node-level for graph-level prediction tasks [55], unlike 2D image classification where pooling layers learn feature vectors for entire images.

**GNNs and 3D point clouds.** The message passing framework in (1) can be used to present a unified ‘geometric’ view of deep learning on non-Euclidean data structures such as 3D point clouds, irregular voxel grids, meshes, and sets [56], [57]. In this work, we consider 3D point cloud networks [58], [59] which process sets of points as nodes. The edges originating from each point are heuristically determined by the  $k$ -nearest neighbors or radius ball queries in the 3D coordinate space. We additionally consider sparse 3D voxel networks [60]–[62] and use trilinear interpolation to convert voxel-level features to point-level features before distillation.

## B. Knowledge Distillation

Knowledge Distillation (KD) transfers *dark knowledge* from high capacity teacher models (which are cumbersome to deploy) to efficient students via matching their output logits in addition to supervised learning. At each node  $i \in \mathcal{V}$ , logit-based KD [29] uses the cross-entropy loss or KL-divergence to match the output logits of the student  $z_i^S$  and teacher  $z_i^T$ , scaled by temperature  $\tau_1$ :

$$\mathcal{L}_{\text{KD}} = \mathcal{H}\left(\text{softmax}\left(\frac{z_i^T}{\tau_1}\right), \text{softmax}\left(\frac{z_i^S}{\tau_1}\right)\right). \quad (2)$$

In this work, we study auxiliary representation distillation techniques that augment or replace logit-based distillation with *representational knowledge* using the teacher and student features,  $f^T \in \mathbb{R}^{d^T}$  and  $f^S \in \mathbb{R}^{d^S}$ , respectively.<sup>1</sup> Our overall objective function for training the student model via the logits as well as latent feature vectors of the teacher is as follows:

$$\mathcal{L} = (1 - \alpha)\mathcal{L}_{\text{SUP}} + \alpha\tau_1^2\mathcal{L}_{\text{KD}} + \beta\mathcal{L}_{\text{Aux}}, \quad (3)$$

where  $\alpha, \beta$  are balancing weights for the logit-based KD and auxiliary representation distillation losses, respectively.

## C. Local Structure Preserving Distillation

We briefly summarize LSP [31], a GNN representation distillation objective which trains the student model to preserve the local structure of graph data from the teacher’s node embedding space. The local structure around each node is defined as the set of parameterized pairwise distances to its neighboring nodes in the latent feature space. The similarity between a pair of linked nodes can be computed by kernel functions (which we tune for):

$$\mathcal{K}(f_i, f_j) = \begin{cases} \|f_i - f_j\|_2^2, & \text{Euclidean distance,} \\ f_i \cdot f_j, & \text{Linear kernel,} \\ (f_i \cdot f_j + c)^d, & \text{Polynomial kernel,} \\ e^{-\frac{1}{2\sigma}\|f_i - f_j\|_2^2}, & \text{RBF kernel.} \end{cases} \quad (4)$$

Thus, the local structure around each node  $i \in \mathcal{V}$  is the softmax probability distribution of the similarities among  $f_i$  and its neighbors’ features  $f_j \forall (i, j) \in \mathcal{E}$ . LSP trains the student model to mimic the local structure from the teacher’s embedding space via KL-divergence:

$$\mathcal{L}_{\text{LSP}} = \mathcal{D}_{\text{KL}}\left(\text{softmax}_{j|(i,j) \in \mathcal{E}}(\mathcal{K}(f_i^S, f_j^S)) \parallel \text{softmax}_{j|(i,j) \in \mathcal{E}}(\mathcal{K}(f_i^T, f_j^T))\right). \quad (5)$$

## D. Global Structure Preserving Distillation

The purely local LSP objective over pre-defined edges may not preserve the global topology of how the teacher embeds the graph, as it does not account for latent interactions among disconnected nodes. In addition to local similarities over edges, we would like to *explicitly* train the student to preserve the global topology in order to better distill representational knowledge from the teacher.

To achieve this, we introduce the Global Structure Preserving loss (GSP), which extends LSP to match *all*  $n^2$  pairwise similarities among node features via mean squared error:

$$\mathcal{L}_{\text{GSP}} = \sum_{j=0}^n \|\mathcal{K}(f_i^T, f_j^T) - \mathcal{K}(f_i^S, f_j^S)\|_2^2. \quad (6)$$

While theoretically more powerful than LSP, GSP may be computationally inefficient and involves two key design choices:

**MSE over KL-divergence** We omit normalizing the similarities via softmax followed by KL-divergence, as this led to very sparse signals over all pairwise similarities when converted to probabilities. We use MSE to match the raw teacher and student pairwise similarity matrices as it worked better empirically.

**Scalability and sub-sampling.** For a set of  $n$  nodes, GSP needs to compute  $n^2$  pairwise similarities for both the teacher and student features. We often need to sub-sample large graphs or 3D point clouds when computing  $\mathcal{L}_{\text{GSP}}$  due to GPU memory constraints instead of storing all possible pairwise similarities. We could have additionally considered triplet-wise relationships as in [46], but found this unscalable to large real-world graphs.

## E. Graph Contrastive Representation Distillation

An alternative to explicit structure preserving techniques such as LSP and GSP is to directly align the node features from the student to those of the teacher. An objective on the features would be a stronger constraint than over pairwise relationships, resulting in *implicitly* preserving relationships over pre-defined as well as latent edges, and thereby preserving global topology. However, we and others [31] found direct feature mimicking approaches [32], [35] from 2D computer vision to be ineffective for GNNs due to mismatch in representational capacity.

Thus, we introduce Graph Contrastive Representation Distillation (G-CRD) which formulates representation distillation as a contrastive learning task on pairwise relationships *across* the teacher and student embedding spaces. Intuitively, we want to maximize the similarity among pairs of student and teacher feature vectors corresponding to the same node, *i.e.*  $f_i^S, f_i^T$  (positive samples), while pushing away the feature vectors of pairs of unmatched nodes, *i.e.*  $f_i^S, f_j^T$  (negative samples). To achieve this, we adapt the InfoNCE objective [37], [39] to the teacher-student paradigm and pose representation distillation as the task of classifying positive pairs among the set of distractors via a temperature-scaled softmax function:

$$\mathcal{L}_{\text{G-CRD}} = -\log \frac{\exp(h(f_i^S, f_i^T)/\tau_2)}{\exp(h(f_i^S, f_i^T)/\tau_2) + \sum_{j \neq i} \exp(h(f_i^S, f_j^T)/\tau_2)}, \quad (7)$$

where  $h: \{d^S, d^T\} \rightarrow [0, 1]$  is a learnt similarity metric, and  $\tau_2$  is a scaler temperature parameter. From an information theoretic perspective, the InfoNCE-style loss aligns the teacher and student embedding spaces by maximizing the mutual information among them. Fig.3 illustrates G-CRD.

G-CRD generalizes Contrastive Representation Distillation [40] from sample-level 2D image classification tasks to fine-grained node-level tasks on graphs, and involves key design choices tailored for GNNs:

<sup>1</sup>Following best practices [34], [40], we consider feature vectors from the penultimate layer before the prediction head for representation distillation.

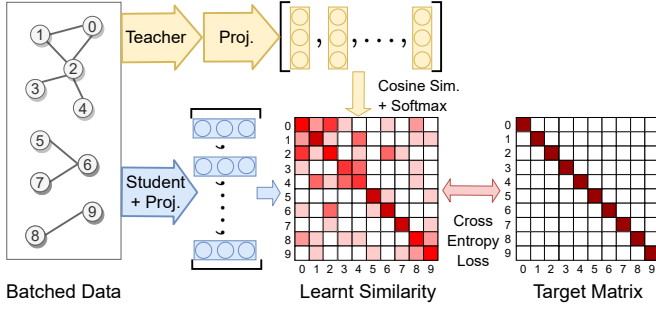


Fig. 3: **Graph Contrastive Representation Distillation.** G-CRD is a node-level contrastive learning task of identifying positive node correspondences across the teacher and student embedding spaces, while pushing away a set of distractor nodes. Here, we define negative samples for each student node feature vector as all the other node features vectors from the teacher within the same mini-batch.

**Structure-aware projection heads.** We define the similarity metric as a learnt cosine similarity between teacher and student features projected to a common representation space:

$$h(f^S, f^T) = \frac{P^S(f^S)' \cdot P^T(f^T)}{\|P^S(f^S)\| \cdot \|P^T(f^T)\|}, \quad (8)$$

where the projection heads  $P^S, P^T$  can be multi-layer perceptrons (MLPs) composed of linear transformations to a common dimension  $d$  (usually that of the student feature) followed by batch normalization and non-linear activation. However, independent MLPs on node feature vectors are ‘structure-agnostic’ [22] – they cannot adapt the shared representation space to the graph structure of the underlying data. Thus, we introduce structure-aware projection heads, which use a single GCN layer [1]<sup>2</sup> followed by batch normalization and non-linear activation:

$$P(f_i) = \begin{cases} \text{GCN}(f_i, f_j | (i, j) \in \mathcal{E}), & \text{Structure-aware,} \\ \text{MLP}(f_i), & \text{Structure-agnostic,} \end{cases} \quad (9)$$

The GCN projection can learn neighborhood-dependent projections via one message passing step, while having the same number of parameters as the structure-agnostic MLP. We tune the choice of projection head as a hyperparameter.

**Node-level contrastive learning.** We formulate G-CRD as a node-level contrastive learning task of identifying positive node correspondences across the teacher and student embedding spaces, while pushing away a set of distractors. G-CRD adapts the well-studied InfoNCE loss in (7). Contrastive Representation Distillation (CRD) [40] is a related representation distillation objective for 2D image classification models:

$$\mathcal{L}_{\text{CRD}} = -\max_h \left( \mathbb{E}_{q(T, S|C=1)} [\log h(T, S)] + N \mathbb{E}_{q(T, S|C=0)} [1 - \log(h(T, S))] \right), \quad (10)$$

where  $T, S$  are random variables for teacher and student features,  $q(T, S|C=1)$  is their joint distribution (positives),  $q(T, S|C=0)$  is their marginal distribution (negatives), and  $h : \{d^S, d^T\} \rightarrow [0, 1]$  is an auxiliary ‘critic’ model which returns an unnormalized similarity score. Crucially, CRD is

tailored for 2D image classification and contrasts among global/per-sample feature vectors. It additionally requires a specialized memory bank [38] to provide a large number  $N$  of negative samples. On the other hand, GNNs build representations at the node-level for both node-level prediction tasks as well as global-level tasks [55]. Thus, it is not possible to directly apply CRD to GNNs beyond graph-level prediction. Our experiments show how a naive application of CRD for GNNs is ineffective, and ablate the impact of our design choices in formulating G-CRD.

**Mini-batch negative sampling.** Contrastive learning among GNN node features from teachers and students alleviates the need for specialized negative sampling procedures: we simply define negative samples for each student node feature as all the other node features from the teacher within the same mini-batch. This is markedly different from recent contrastive pre-training objectives for GNNs, which rely on handcrafted data augmentation [18], [19] or sub-graph sampling procedures [20], [21] to generate multiple views of graphs.

Unlike sample-level CRD, our approach does not require extremely large batch sizes or negative samples, as the combined cardinality of all nodes within a mini-batch is sufficient for boosting student performance. G-CRD is robust across a range of graph and batch sizes – from 25 nodes per graph in mini-batches of 32, up to single giant graphs with over 1.9 million nodes.

## IV. EXPERIMENTAL SETUP

### A. Datasets

We benchmark distillation techniques across a range of tasks on single large-scale networks, batches of small graphs, as well as batches of 3D point clouds, summarized in Tab.I. As we are motivated by real-world and real-time applications involving noisy and shifting data distributions, we make the following considerations for our benchmarks:

**Challenging for student models.** Past work on distillation for GNNs [31] used small-scale PPI [2] (node classification) and ModelNet [66] (3D point cloud classification), both of which are considered saturated by the community [11], [67]. The performance gap between cumbersome teachers and lightweight student models is negligible for these datasets, which makes them unsuitable benchmarks for comparing techniques. (See the Appendix for an investigation on PPI.)

We evaluate node classification on ARXIV and the Microsoft Academic Graph (MAG) [11], [65], which are  $70\times$  and  $800\times$  larger than PPI, respectively, and consider the more challenging semantic segmentation task on 3D point cloud scenes from S3DIS [41] that are over  $10\times$  denser than CAD object scans from ModelNet. We additionally evaluate graph classification on MOLHIV from OGB/MoleculeNet [64].

**Out-of-distribution evaluation.** Unlike PPI and ModelNet, all datasets involve realistic and carefully curated train-test splitting procedures to evaluate out-of-distribution generalization. ARXIV and MAG follow a temporal split, MOLHIV trains on common molecular scaffolds while testing on rare ones, and S3DIS is split according to 6 distinct areas.

<sup>2</sup>We chose GCN as it is one of the most well studied and lightweight layers.

TABLE I: **Summary of datasets.** ARXIV, MAG, and MOLHIV were accessed via OGB [11] and S3DIS via PyTorch Points 3D [63].

Name	#Samples	Avg. #Nodes	Avg. #Edges	Split Scheme	Split Ratio	Prediction	Task	Metric
MOLHIV [64]	41,127	25.5	27.5	Scaffold	80/10/10	Graph-level	Binary clf.	ROC-AUC
S3DIS [41]	5,845	20,000	-	Rooms	52/19/29	Point-level	Multi-class clf. (16)	mIoU, mAcc
ARXIV [11]	1	169,343	1,166,243	Time	54/18/28	Node-level	Multi-class clf. (40)	Accuracy
MAG [65]	1	1,939,743	21,111,007	Time	85/9/6	Node-level	Multi-class clf. (349)	Accuracy
PPI [2]	24	2,372	34,113	Random	84/8/8	Node-level	Multi-label (128) Binary clf.	F1

TABLE II: **Summary of teacher and student model architectures.** Peak GPU usage and average inference latency are reported over test set graphs with fixed batch size 1 with single-threading on a single GPU (RTX3090 for ARXIV/MAG, V100 for MOLHIV/S3DIS). For MAG, we exclude 136,440,832 extra embedding dictionary parameters from #Param. and their lookup time in L.Time.

Name	Type	#Layer, #Hidden	#Parameters	Peak GPU Usage	Average L.Time	
MOLHIV	GIN-E [18]	Teacher	5,300	3,336,306	1.2GB	9ms
	PNA [16]	Teacher	5,150	2,433,901	1.2GB	18ms
	GCN [1]	Student	2,100	40,801	1.1GB	4ms ( $\downarrow 78\%$ )
	GIN [14]	Student	2,50	10,951	1.1GB	2ms ( $\downarrow 89\%$ )
S3DIS	SPVCNN [61]	Teacher	U-Net	21,777,421	1.8GB	88ms
	KP-FCNN [59]	Teacher	U-Net	14,082,688	4.8GB	227ms
	PointNet++ [58]	Student	U-Net, SSG	1,400,269	1.2GB	22ms ( $\downarrow 90\%$ )
	MinkNet [60]	Student	U-Net, 20%cr.	852,512	1.2GB	81ms ( $\downarrow 64\%$ )
ARXIV	GAT [4]	Teacher	3,750	1,441,580	6.8GB	93ms
	GCN [1]	Student	2,256	43,816	2.2GB	11ms ( $\downarrow 88\%$ )
	GraphSage [2]	Student	2,256	86,824	2.1GB	5ms ( $\downarrow 95\%$ )
	SIGN [22]	Student	3,512	3,566,128	9.3GB	5ms ( $\downarrow 95\%$ )
MAG	R-GCN [68]	Teacher	3,512	5,575,540	20.8GB	189ms
	R-GCN [68]	Student	2,32	169,428	11.1GB	134ms ( $\downarrow 29\%$ )

### B. Teacher and Student Architectures

Tab.II summarizes our choice of teachers and students, which are made with the following considerations about deploying GNNs: (1) *depth* – more message passing rounds allow models to access larger sub-graphs around each node, at the cost of training and inference time; (2) *hidden channels* – especially for giant graphs, increasing hidden channels boosts performance as well as memory consumption, and may require specialized sampling procedures; and (3) *architectural complexity* – principled geometric priors [59] or attention mechanisms over edges [4], [16] improve model expressivity but tend to have higher inference latency and memory usage.

Unlike in [31], we benchmark distillation techniques across *heterogeneous* architecture families with significant mismatch in terms of parameter count, expressive power, and inference time; *e.g.* for social networks, we distil from Graph Attention Networks [4] to simple GCNs [1]. For 3D point clouds, we distil from Kernel Point ConvNet [59] teachers to lightweight PointNet++ [58] and voxel-based MinkowskiNet [60]. We give further rationale for our choice of teacher-student pairs for each experiment in Sec.V.

### C. Training and Evaluation

Our implementation is built upon PyTorch Geometric [69], PyTorch Points 3D [63], and Open Graph Benchmark [11]. We follow the best practices and guidelines for each dataset.

**Training.** Teacher models are trained via the conventional supervised learning paradigm and the final weights for distillation are selected by early stopping. Student models are trained via the knowledge distillation pipeline described in Sec.III. For the OGB datasets, we follow their example implementations and training setups for both teacher and student models. For

S3DIS, the teacher models are trained for 600 epochs following their original learning rate strategies, while the student models are trained for 300 epochs and use an exponential learning rate strategy. We use the conventional data preparation and augmentation procedures for S3DIS via PyTorch Points 3D.

**Evaluation.** For the OGB datasets, we use the official evaluators and report the average test performance across 8/10 random seeds (each teacher-student pair is re-trained for each seed). For S3DIS, we follow best practices in the literature: all models are trained once, and we report the average mIoU and mAcc over 10 voting runs on the held-out Area-5 test set using the evaluation protocol from PyTorch Points 3D.

**Baselines and hyperparameters.** Following Yang et al. [31], we compare the GNN representation distillation techniques G-CRD, GSP and LSP to logit-based KD [29] (2) as well as FitNet [32] and Attention Transfer (AT) [35], two feature mimicking baselines adapted from 2D computer vision which are formulated as:  $\mathcal{L}_{\text{Aux}} = \|P^T(f_i^T) - P^S(f_i^S)\|_2^2$  (FitNet uses L2 normalized projection head, AT uses attention mapping).

We tune the loss balancing weights  $\alpha, \beta$  in (3) for all techniques on the validation set. For KD, we tune  $\alpha \in \{0.8, 0.9\}$ ,  $\tau_1 \in \{4, 5\}$ . For FitNet, AT, LSP, and GSP, we tune  $\beta \in \{100, 1000, 10000\}$  and the kernel in (4) (only LSP, GSP). For G-CRD, we tune  $\beta \in \{0.01, 0.05\}$ ,  $\tau_2 \in \{0.05, 0.075, 0.1\}$  and the projection head in (9). When comparing representation distillation methods, we set  $\alpha$  to 0 in order to ablate performance, as in [40], and reduce  $\beta$  by one order of magnitude.

## V. RESULTS

### A. Molecular Graph Property Prediction

We consider the graph-level property prediction task over batches of molecular graphs. Reducing the inference latency of GNNs for molecules speeds up high throughput virtual screening [64]. Additionally, virtual screening on proprietary data will require homomorphically encrypted models, which further demand low layer count and hidden size [70]. As teachers, we consider 5-layer deep GIN-E [18] and PNA [16] augmented with virtual nodes, two strong OGB baselines. Notably, PNA is the most expressive message passing GNN but explicitly materializes messages over graph edges, leading to higher memory requirement and inference latency. Our student architectures are 2-layer GCN [1] and GIN [14], which are comparatively less expressive and do not use virtual nodes (and edge features in GIN), while having low inference latency.

In Tab.III, we compare logit-based KD and the representation distillation techniques across a range of teacher-student pairs. **We find that the implicit G-CRD technique consistently improves over the supervised student’s performance and**

TABLE III: **Molecular graph classification on MOLHIV** (metric: ROC-AUC (%)). **Bold/underlined** denote the best/second best performing distillation technique for each column. The arrows ( $\uparrow$ )/( $\downarrow$ ) denote performance improvement/regression compared to logit-based Knowledge Distillation (KD). We report the average performance and std. across 8 random seeds.

Teacher (#Layer,#Param):		GIN-E (5L,3.3M)	PNA (5L,2.4M)	GIN-E (5L,3.3M)	PNA (5L,2.4M)	PNA (5L,2.4M)
Student (#Layer,#Param):		GCN (2L,15K)	GCN (2L,15K)	GCN (2L,40K)	GCN (2L,40K)	GIN (2L,10K)
Sup.	Supervised Teacher	77.69 $\pm$ 1.61	77.48 $\pm$ 1.71	77.69 $\pm$ 1.61	77.48 $\pm$ 1.71	77.48 $\pm$ 1.71
	Supervised Student	73.02 $\pm$ 1.46	73.02 $\pm$ 1.46	73.65 $\pm$ 1.50	73.65 $\pm$ 1.50	73.03 $\pm$ 2.02
Distillation	KD [29]	<u>74.08</u> $\pm$ 1.03	<u>74.13</u> $\pm$ 1.72	<u>75.25</u> $\pm$ 1.71	74.45 $\pm$ 1.27	73.42 $\pm$ 2.14
	FitNet [32]	73.62 $\pm$ 1.05 ( $\downarrow$ )	73.65 $\pm$ 1.25 ( $\downarrow$ )	74.52 $\pm$ 1.33 ( $\downarrow$ )	74.39 $\pm$ 1.46 ( $\downarrow$ )	72.88 $\pm$ 0.89 ( $\downarrow$ )
	AT [35]	73.85 $\pm$ 0.85 ( $\downarrow$ )	73.64 $\pm$ 1.50 ( $\downarrow$ )	74.94 $\pm$ 0.97 ( $\downarrow$ )	73.89 $\pm$ 1.92 ( $\downarrow$ )	<u>73.87</u> $\pm$ 2.28 ( $\uparrow$ )
	LSP [31]	73.58 $\pm$ 1.29 ( $\downarrow$ )	73.24 $\pm$ 1.67 ( $\downarrow$ )	75.04 $\pm$ 1.20 ( $\downarrow$ )	74.43 $\pm$ 1.58 ( $\downarrow$ )	70.74 $\pm$ 1.82 ( $\downarrow$ )
	GSP (Ours)	72.83 $\pm$ 1.30 ( $\downarrow$ )	73.74 $\pm$ 0.93 ( $\downarrow$ )	75.12 $\pm$ 1.27 ( $\downarrow$ )	<u>75.09</u> $\pm$ 1.48 ( $\uparrow$ )	69.68 $\pm$ 2.88 ( $\downarrow$ )
	G-CRD (Ours)	<b>74.34</b> $\pm$ 1.44 ( $\uparrow$ )	<b>75.11</b> $\pm$ 0.73 ( $\uparrow$ )	<b>75.53</b> $\pm$ 1.64 ( $\uparrow$ )	<b>75.89</b> $\pm$ 0.80 ( $\uparrow$ )	<b>75.77</b> $\pm$ 2.02 ( $\uparrow$ )

TABLE IV: **3D Semantic segmentation on S3DIS** (metric: mIoU, mAcc). **Bold/underlined** denote the best/second best performing distillation technique for each column. The arrows ( $\uparrow$ )/( $\downarrow$ ) denote performance improvement/regression compared to logit-based Knowledge Distillation (KD). We report the average performance over 10 voting runs.

Teacher (#Param):		KP-FCNN (14.0M)	SPVCNN (21.8M)	KP-FCNN (14.0M)	SPVCNN (21.8M)
Student (#Param):		PointNet, SSG (1.4M)	PointNet, SSG (1.4M)	MinkNet, 20% cr. (0.8M)	MinkNet, 20% cr. (0.8M)
Sup.	Supervised Teacher	62.70, 69.54	64.58, 71.71	62.70, 69.54	64.58, 71.71
	Supervised Student	49.67, 57.51	49.67, 57.51	55.29, 64.14	55.29, 64.14
Distillation	KD [29]	51.89, 59.48	<u>51.81</u> , <u>59.22</u>	56.00, 64.90	55.78, 64.51
	FitNet [32]	49.37, 57.35 ( $\downarrow$ )	49.85, 57.78 ( $\downarrow$ )	48.94, 57.26 ( $\downarrow$ )	53.62, 63.14 ( $\downarrow$ )
	AT [35]	51.82, 59.38 ( $\downarrow$ )	49.57, 57.13 ( $\downarrow$ )	56.02, 64.87 ( $\uparrow$ )	54.84, 63.78 ( $\downarrow$ )
	LSP [31]	50.69, 58.49 ( $\downarrow$ )	51.07, 58.57 ( $\downarrow$ )	54.20, 63.59 ( $\downarrow$ )	55.20, 64.34 ( $\downarrow$ )
	GSP (Ours)	53.00, 61.15 ( $\uparrow$ )	51.68, 60.35 ( $\downarrow$ )	55.50, 65.19 ( $\downarrow$ )	54.77, 63.88 ( $\downarrow$ )
	G-CRD (Ours)	<b>53.15</b> , <b>61.15</b> ( $\uparrow$ )	<b>53.27</b> , <b>61.29</b> ( $\uparrow$ )	<b>56.07</b> , <b>64.87</b> ( $\uparrow$ )	<b>55.83</b> , <b>65.03</b> ( $\uparrow$ )

**outperforms the explicit global structure preserving approach, GSP. In turn, GSP outperforms the purely local approach, LSP.** While all other distillation techniques do offer minor performance boosts over the supervised student, G-CRD is the only one which improves over the KD baseline for most teacher-student combinations.

### B. 3D Point Cloud Semantic Segmentation

Semantic segmentation of 3D scene graphs is a safety critical real-time task with applications in autonomous driving and robotics. Models process 3D scenes as sets of points or voxel grids, and make a dense prediction by assigning semantic categories to each point/unit. Recent state-of-the-art architectures involve strong geometric priors and complex architectures, leading to increased inference latency and GPU memory requirement. Here, we consider distilling two powerful models, Kernel Point Convolution (KP-FCNN, rigid kernel) [59] and Sparse Point-Voxel CNN (SPVCNN) [61], [62], into simpler models with low inference latency and memory usage: PointNet++ with single-scale grouping [58] and voxel-based MinkowskiNet [60] at low 20% channel ratio.

In Tab.IV, we see trends that are consistent with the previous section: G-CRD consistently improves the performance of lightweight students compared to GSP, and is particularly effective for boosting PointNet++. **Notably, due to a large mismatch in teacher-student representation capacity, feature mimicking losses, FitNet and AT, may worsen the student’s performance over purely supervised learning.**

### C. Node Classification on Social Networks

Reducing model depth and feature dimensions boosts inference and reduces memory usage for real-time applications on large-scale graphs. For ARXIV, a homogeneous citation network where models classify the subject of each node/paper, we use a strong 3-layer GAT [4] teacher. GAT has high memory requirement during training and inference due to its attention mechanism. We distil into 2-layer GCN [1] and GraphSage [2], which are comparatively more scalable but lack the expressivity of attention. We also distil to structure-agnostic SIGN [22] designed for parallelized large-graph processing. LSP cannot be used for SIGN as it does not make use of graph structure.

Experiments on the giant heterogeneous Microsoft Academic Graph (MAG) of authors, papers, and institutions further tests the scalability of distillation. We distil among Relational-GCNs [68] at different depth and feature sizes. We use the GraphSAINT [73] sampler to fit GPU memory.

In Tab.V, when considering each technique independently, logit-based KD is the best while G-CRD is the second best. We believe this can be explained by the homophily phenomenon for node labels on social networks [74]. The soft labels from the teacher model thus providing a more informative signal for knowledge transfer than the latent representations. On combining KD with representation distillation, KD + G-CRD consistently outperforms all other pairs. **GSP is the worst performing technique for MAG, demonstrating the inability of explicit global topology preservation to scale to large graphs.** Note that performance gains from distillation may seem marginal, but are significant as metrics are averaged over several thousand nodes (48K for ARXIV, 42K for MAG).

TABLE V: **Node classification on ARXIV and MAG** (metric: Accuracy (%)). **Bold/underlined** denote the best/second best performing distillation technique for each column. The arrows ( $\uparrow$ )/( $\downarrow$ ) denote performance improvement/regression compared to logit-based Knowledge Distillation (KD). We report the average performance and std. across 10 random seeds.

		Dataset:		ARXIV	ARXIV	ARXIV	MAG
		Teacher (#Layer,#Param):	GAT (3L,1.4M)	GAT (3L,1.4M)	GAT (3L,1.4M)	GAT (3L,1.4M)	R-GCN (3L,5.5M)
		Student (#Layer,#Param):	GCN (2L,44K)	GraphSage (2L,87K)	SIGN (3L,3.5M)	SIGN (3L,3.5M)	R-GCN (2L,170K)
Sup.	Supervised Teacher		73.91 $\pm$ 0.12	73.91 $\pm$ 0.12	73.91 $\pm$ 0.12	73.91 $\pm$ 0.12	49.48 $\pm$ 0.35
	Supervised Student		71.25 $\pm$ 0.28	70.97 $\pm$ 0.23	71.98 $\pm$ 0.16	71.98 $\pm$ 0.16	46.22 $\pm$ 0.31
Distillation	KD [29]		<u>71.55</u> $\pm$ 0.25	<b>71.44</b> $\pm$ 0.10	<b>72.26</b> $\pm$ 0.11	<b>72.26</b> $\pm$ 0.11	<b>46.65</b> $\pm$ 0.20
	FitNet [32]		71.38 $\pm$ 0.17 ( $\downarrow$ )	70.78 $\pm$ 0.25 ( $\downarrow$ )	71.98 $\pm$ 0.13 ( $\downarrow$ )	71.98 $\pm$ 0.13 ( $\downarrow$ )	46.15 $\pm$ 0.24 ( $\downarrow$ )
	AT [35]		70.44 $\pm$ 0.28 ( $\downarrow$ )	70.17 $\pm$ 0.11 ( $\downarrow$ )	71.99 $\pm$ 0.14 ( $\downarrow$ )	71.99 $\pm$ 0.14 ( $\downarrow$ )	46.09 $\pm$ 0.27 ( $\downarrow$ )
	LSP [31]		71.52 $\pm$ 0.22 ( $\downarrow$ )	70.95 $\pm$ 0.22 ( $\downarrow$ )	-	-	46.23 $\pm$ 0.41 ( $\downarrow$ )
	GSP (Ours)		71.41 $\pm$ 0.31 ( $\downarrow$ )	70.98 $\pm$ 0.33 ( $\downarrow$ )	71.99 $\pm$ 0.12 ( $\downarrow$ )	71.99 $\pm$ 0.12 ( $\downarrow$ )	46.04 $\pm$ 0.15 ( $\downarrow$ )
	G-CRD (Ours)		<b>71.64</b> $\pm$ 0.16 ( $\uparrow$ )	<u>71.15</u> $\pm$ 0.12 ( $\downarrow$ )	<u>72.10</u> $\pm$ 0.10 ( $\downarrow$ )	<u>72.10</u> $\pm$ 0.10 ( $\downarrow$ )	<u>46.42</u> $\pm$ 0.20 ( $\downarrow$ )
KD + Dist.	KD + FitNet [32]		71.10 $\pm$ 0.19 ( $\downarrow$ )	71.11 $\pm$ 0.17 ( $\downarrow$ )	<u>72.31</u> $\pm$ 0.08 ( $\uparrow$ )	<u>72.31</u> $\pm$ 0.08 ( $\uparrow$ )	46.60 $\pm$ 0.36 ( $\downarrow$ )
	KD + AT [35]		70.91 $\pm$ 0.31 ( $\downarrow$ )	71.06 $\pm$ 0.19 ( $\downarrow$ )	<u>72.27</u> $\pm$ 0.11 ( $\uparrow$ )	<u>72.27</u> $\pm$ 0.11 ( $\uparrow$ )	46.59 $\pm$ 0.41 ( $\downarrow$ )
	KD + LSP [31]		71.35 $\pm$ 0.23 ( $\downarrow$ )	71.34 $\pm$ 0.17 ( $\downarrow$ )	-	-	<u>46.73</u> $\pm$ 0.31 ( $\uparrow$ )
	KD + GSP (Ours)		71.39 $\pm$ 0.19 ( $\downarrow$ )	<u>71.51</u> $\pm$ 0.18 ( $\uparrow$ )	<u>72.27</u> $\pm$ 0.16 ( $\uparrow$ )	<u>72.27</u> $\pm$ 0.16 ( $\uparrow$ )	46.49 $\pm$ 0.18 ( $\downarrow$ )
	KD + G-CRD (Ours)		<b>71.57</b> $\pm$ 0.23 ( $\uparrow$ )	<b>71.59</b> $\pm$ 0.15 ( $\uparrow$ )	<b>72.32</b> $\pm$ 0.11 ( $\uparrow$ )	<b>72.32</b> $\pm$ 0.11 ( $\uparrow$ )	<b>46.78</b> $\pm$ 0.32 ( $\uparrow$ )

TABLE VI: **Topological similarity measures among teacher and student embeddings on ARXIV**. We report average metrics across 10 random seeds for teacher and student validation set node embeddings. CKA Score (range: [0, 1]) measures global representational similarity between embedding sets. Global Mantel Test (range: [-1, 1]) measures Pearson correlation between the pairwise cosine distance matrices of embedding sets, *i.e.* all pairwise relationships or global structural similarity. Local Mantel Test measures local structural similarity by only considering distances over pre-defined edges. **Bold/underlined/italics** denote the highest/second/third highest similarity for each column.

Similarity Metric:	CKA Score [71]		Global Mantel Test [72]		Local Mantel Test [72]	
	Teacher (#Layer,#Param):	GAT (3L,1.4M)				
	Student (#Layer,#Param):	GCN (2L,44K)	GraphSage (2L,87K)	GCN (2L,44K)	GraphSage (2L,87K)	GCN (2L,44K)
Sup. Teacher		1.000 $\pm$ 0.000				
Sup. Student		0.655 $\pm$ 0.011	0.609 $\pm$ 0.007	0.680 $\pm$ 0.011	0.623 $\pm$ 0.008	0.695 $\pm$ 0.005
KD [29]		0.716 $\pm$ 0.011	0.721 $\pm$ 0.003	0.733 $\pm$ 0.007	0.730 $\pm$ 0.004	0.710 $\pm$ 0.006
KD + FitNet [32]		0.740 $\pm$ 0.006	<b>0.764</b> $\pm$ 0.005	<b>0.760</b> $\pm$ 0.005	<b>0.765</b> $\pm$ 0.005	0.736 $\pm$ 0.008
KD + AT [35]		0.570 $\pm$ 0.020	0.696 $\pm$ 0.013	0.593 $\pm$ 0.015	0.687 $\pm$ 0.012	0.669 $\pm$ 0.009
KD + LSP [31]		0.714 $\pm$ 0.006	0.708 $\pm$ 0.005	0.697 $\pm$ 0.011	0.683 $\pm$ 0.005	<b>0.772</b> $\pm$ 0.006
KD + GSP (Ours)		<b>0.746</b> $\pm$ 0.010	<u>0.752</u> $\pm$ 0.004	<u>0.756</u> $\pm$ 0.006	<u>0.757</u> $\pm$ 0.003	0.722 $\pm$ 0.007
KD + G-CRD (Ours)		0.725 $\pm$ 0.007	<u>0.727</u> $\pm$ 0.003	<u>0.750</u> $\pm$ 0.004	<u>0.753</u> $\pm$ 0.003	<u>0.742</u> $\pm$ 0.004

#### D. Does Distillation Preserve Topology?

Across Tab.III, V, IV, we observe that G-CRD, which implicitly preserves global topology from the teacher to the student embedding space, outperforms explicit structure preserving approaches LSP and GSP, as well as feature mimicking baselines FitNet and AT. In order to unpack the efficacy of G-CRD beyond performance metrics, we measure how well distillation techniques preserve both global and local topology from the teacher to the student node embedding space in Tab.VI. To quantify global representational similarity between the teacher and student, we use the recently proposed Centered Kernel Alignment score (CKA) [71], [75] between two embedding sets, as well as the classical Mantel Test [72], [76]<sup>3</sup> of Pearson correlation between all pairwise cosine distances from two embedding sets (as in the GSP loss). Additionally, we quantify local structural similarity via another Mantel Test which only considers distances over pre-defined edges (as in the LSP loss).

Our results largely follow the intuitions developed in Fig.2: In terms of global topology and representational similarity, students trained with FitNet, GSP, and G-CRD have high correlations to the teacher. On the other hand, LSP is the

most correlated for local topology over existing graph edges, but relatively poorer at preserving global topology. **Overall, we see that the implicit contrastive approach G-CRD strikes a balance between preserving both local and global relationships, while the explicit LSP/GSP are best at preserving only one or the other.**

#### E. Ablation Study of Contrastive Loss Design

This section highlights the key design choices that distinguish G-CRD from Contrastive Representation Distillation (CRD) [40], which introduced a contrastive distillation objective for 2D image classification. CRD is specialized for global per-sample level tasks: it contrasts linearly projected global representations and uses the loss in (10). On the other hand, G-CRD performs contrastive learning at the node-level using an InfoNCE-style loss (7) and a specialized projection head design (9); it is flexible to handle both node and global-level tasks.

In Tab.VII, we compare G-CRD and our adaptation of CRD to GNNs. In the first set of rows, we see that contrasting representations at the node-level (as in G-CRD) significantly outperforms global-level contrastive learning (as in CRD) as well as sample-wise node-level (only contrasting among nodes belonging to the same sample). In the second set of rows, we find that the G-CRD loss outperforms the CRD objective across

<sup>3</sup>We use the implementation from scikit-bio (skbio.stats.distance.mantel).

TABLE VII: Ablation study for contrastive loss design (metric: ROC-AUC (%) for MOLHIV; Accuracy (%) for ARXIV).

Repr.	Loss	Dataset:			
		Proj.	MOLHIV PNA (2.4M) GCN (15K)	MOLHIV PNA (2.4M) GCN (40K)	ARXIV GAT (1.4M) GCN (44K)
Nodes	$\mathcal{L}_{G-CRD}$	MLP	74.72 $\pm$ 0.64	75.47 $\pm$ 0.79	71.56 $\pm$ 0.13
Nodes (s.w.)	$\mathcal{L}_{G-CRD}$	MLP	74.09 $\pm$ 1.65	74.74 $\pm$ 0.86	N.A.
Global	$\mathcal{L}_{G-CRD}$	MLP	73.32 $\pm$ 1.24	73.87 $\pm$ 1.43	N.A.
Nodes	$\mathcal{L}_{G-CRD}$	MLP	74.72 $\pm$ 0.64	75.47 $\pm$ 0.79	71.56 $\pm$ 0.13
Nodes	$\mathcal{L}_{CRD}$	MLP	73.62 $\pm$ 1.97	75.20 $\pm$ 1.18	71.48 $\pm$ 0.15
Nodes	$\mathcal{L}_{G-CRD}$	GCN	75.11 $\pm$ 0.73	75.89 $\pm$ 0.80	71.64 $\pm$ 0.16
Nodes	$\mathcal{L}_{G-CRD}$	MLP	74.72 $\pm$ 0.64	75.47 $\pm$ 0.79	71.56 $\pm$ 0.13
Full G-CRD: Nodes + $\mathcal{L}_{G-CRD}$		+ GCN Proj.	75.11 $\pm$ 0.73	75.89 $\pm$ 0.80	71.64 $\pm$ 0.16
Full CRD: Global + $\mathcal{L}_{CRD}$		+ Lin. Proj.	73.67 $\pm$ 1.55	73.37 $\pm$ 2.08	N.A.

TABLE VIII: Molecular graph classification on MOLHIV under INT8 quantization aware training (metric: ROC-AUC (%)).

Teacher (#Param):		PNA @FP32 (2.4M)	PNA @FP32 (2.4M)
Student (#Param):		GIN @INT8 (10K)	GIN @INT8 (10K)
Training Scheme:		Vanilla QAT	DegreeQuant [28]
Sup.	Teacher	77.48 $\pm$ 1.71	77.48 $\pm$ 1.71
	Student	70.62 $\pm$ 3.05	71.38 $\pm$ 2.38
Distillation	KD [29]	72.93 $\pm$ 1.14	71.74 $\pm$ 1.97
	FitNet [32]	73.03 $\pm$ 1.89 ( $\uparrow$ )	71.08 $\pm$ 3.86 ( $\downarrow$ )
	AT [35]	72.76 $\pm$ 1.02 ( $\downarrow$ )	69.31 $\pm$ 2.12 ( $\downarrow$ )
	LSP [31]	70.91 $\pm$ 2.23 ( $\downarrow$ )	68.94 $\pm$ 4.23 ( $\downarrow$ )
	GSP (Ours)	66.44 $\pm$ 4.06 ( $\downarrow$ )	68.84 $\pm$ 2.29 ( $\downarrow$ )
	G-CRD (Ours)	73.65 $\pm$ 2.09 ( $\uparrow$ )	73.50 $\pm$ 1.13 ( $\uparrow$ )

graph as well as node-level tasks when fixing the contrastive learning at the node-level. In the third set of rows, we show that the structure-aware GCN projection head boosts performance over a structure-agnostic MLP projection. Finally, we show that the full G-CRD implementation consistently outperforms a naive CRD implementation at graph-level tasks.

### F. Quantizability of Distilled Representations

Quantization of model weights and activations to lower precision arithmetic is a complementary compression technique to distillation. Models at lower precision such as 8-bit integers have significantly faster inference latency and lower memory usage. However, quantization aware training (QAT) is known to degrade performance. In Tab.VIII, we explore whether distillation can improve the performance of a lightweight quantized 2-layer GIN model when trained with vanilla QAT as well as DegreeQuant [28], a GNN-specific QAT. We find that QAT with G-CRD enables quantized models to retain a large portion of their performance at 8-bit integer precision as compared to other distillation techniques. Significantly, GIN trained with G-CRD at INT8 (73.65% ROC-AUC) can still outperform its purely supervised counterpart at full 32-bit floating point precision (73.03%, see column 6 in Tab.III).

G-CRD is well suited for QAT because the projection heads ensure that contrastive distillation take place at full precision even when the student model is at low INT8 (the heads do not interfere with the inference phase, which always uses INT8). On the other hand, structure preserving approaches LSP and GSP are particularly ill suited as they match relationships from low INT8 feature vectors (student) to full precision (teacher).

TABLE IX: Molecular graph classification/regression on small-scale MOL\* datasets (metric: ROC-AUC (%) for BACE, SIDER; MSE for ESOL). We perform linear probing on frozen node representations from GCN (2L,40K) initialized randomly or pre-trained on MOLHIV via supervised learning or various distillation techniques.

Initialization	MOLBACE	MOLSIDER	MOLESOL
Random	67.03 $\pm$ 1.63	55.35 $\pm$ 1.05	2.097 $\pm$ 0.128
Supervised	71.32 $\pm$ 2.48	58.40 $\pm$ 1.18	1.907 $\pm$ 0.064
KD [29]	72.24 $\pm$ 2.38	59.50 $\pm$ 0.73	1.948 $\pm$ 0.084
FitNet [32]	71.82 $\pm$ 4.17 ( $\downarrow$ )	57.31 $\pm$ 1.13 ( $\downarrow$ )	2.032 $\pm$ 0.137 ( $\downarrow$ )
AT [35]	69.73 $\pm$ 3.57 ( $\downarrow$ )	57.62 $\pm$ 0.43 ( $\downarrow$ )	1.820 $\pm$ 0.062 ( $\uparrow$ )
LSP [31]	70.03 $\pm$ 2.12 ( $\downarrow$ )	58.67 $\pm$ 0.71 ( $\downarrow$ )	1.998 $\pm$ 0.058 ( $\downarrow$ )
GSP (Ours)	70.53 $\pm$ 1.74 ( $\downarrow$ )	58.57 $\pm$ 1.13 ( $\downarrow$ )	1.948 $\pm$ 0.070 ( $\uparrow$ )
G-CRD (Ours)	72.46 $\pm$ 2.19 ( $\uparrow$ )	56.81 $\pm$ 1.42 ( $\downarrow$ )	1.812 $\pm$ 0.112 ( $\uparrow$ )

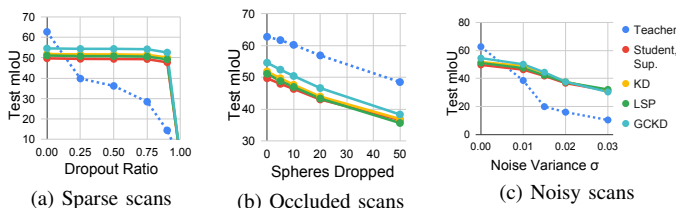


Fig. 4: Robustness analysis for 3D semantic segmentation.

### G. Transferability of Distilled Representations

In biomedical discovery, we are interested in models’ ability to generalize or extrapolate to unseen regions of chemical space. In addition to evaluating on out-of-distribution molecular scaffolds from MOLHIV’s test set, we further test the transferability of distilled models on smaller scale molecule datasets from OGB: MOLBACE (1,513 samples), MOLSIDER (1,427 samples), and MOLESOL (1,128 samples) in Tab.IX. We perform linear probing on frozen node features from a 2-layer GCN model. The GCN feature extractor can either be initialized randomly, pre-trained on MOLHIV via supervised learning, or pre-trained via various distillation techniques with a 5-layer PNA teacher. Encouragingly, we find that distillation leads to more transferable representations than random or purely supervised initialization. Overall, G-CRD boosts the transferability of student models for 2 out of 3 datasets with structurally different molecules as well as task semantics.

### H. Robustness of Distilled Representations

Beyond clean test set performance, lightweight 3D segmentation models often have to deal with ‘dirty’ data such as sparse, occluded or noisy scans. In Fig.4, we evaluate the impact of distillation on the robustness of PointNet++ across three common challenging scenarios (we also show the KP-FCNN teacher for comparison): (1) *Sparse scans* – randomly dropout a percentage of points for each scan; (2) *Partial and occluded scans* – dropout all points sampled within a number of random spheres of fixed radius of 0.5m for each scan; and (3) *Noisy scans* – add independent random noise to the 3D coordinates of each point with a variance factor  $\sigma$ .

Training the lightweight student with G-CRD consistently improves its robustness compared to purely supervised training as well as logit-based KD [29] and LSP [31]. Promisingly,

lightweight students can be more robust to sparse or noisy scans than cumbersome teachers.

## VI. CONCLUSION

In this work, we study representation distillation for GNNs from the perspective of training the student to preserve global topology from the teacher’s node embedding space. We develop two new approaches to do so: (1) An explicit approach termed Global Structure Preserving loss (GSP), which extends the previously proposed Local Structure Preserving loss (LSP) [31]; and (2) An implicit approach, Graph Contrastive Representation Distillation (G-CRD), the first contrastive distillation technique specialized for GNNs.

Additionally, we introduce an expanded set of benchmarks on large-scale real-world datasets where the performance gap between teacher and student GNNs is non-negligible. This was missing from the LSP study which used synthetic and saturated datasets. Our experiments reveal that training lightweight GNN models with G-CRD consistently improves their performance, robustness, and quantizability compared to explicit structure preserving approaches (LSP, GSP) as well as baselines adapted from 2D computer vision. We further unpack the efficacy of G-CRD over GSP and LSP through the lens of representational similarity of teacher and student embedding spaces.

Currently, knowledge distillation techniques for GNNs are neither as effective nor as well understood as their counterparts in 2D computer vision. We hope that our techniques, benchmarks and open-source codebase can form the basis for comparison in future work on this emerging research direction.

## ACKNOWLEDGEMENTS

This research is supported by the Agency for Science, Technology and Research (A\*STAR) under its AME Programmatic Funds (Project No.A19E3b0099 and Project No. A20H6b0151). We would like to thank Efe Camci, Vijay Prakash Dwivedi, Yoon Ji Wei, Edwin Khoo, Hannes Stärk, Shyam A. Tailor and Wanyue Zhang for helpful comments and discussions.

## REFERENCES

- [1] T. N. Kipf and M. Welling, “Semi-supervised classification with graph convolutional networks,” in *ICLR*, 2017.
- [2] W. L. Hamilton, R. Ying, and J. Leskovec, “Inductive representation learning on large graphs,” in *NeurIPS*, 2017.
- [3] Y. Wang, Y. Sun, Z. Liu, S. E. Sarma, M. M. Bronstein, and J. M. Solomon, “Dynamic graph cnn for learning on point clouds,” *ACM TOG*, 2019.
- [4] P. Veličković, G. Cucurull, A. Casanova, A. Romero, P. Liò, and Y. Bengio, “Graph Attention Networks,” *ICLR*, 2018.
- [5] P. W. Battaglia, J. B. Hamrick, V. Bapst, A. Sanchez-Gonzalez, V. Zambaldi, M. Malinowski, A. Tacchetti, D. Raposo, A. Santoro, R. Faulkner *et al.*, “Relational inductive biases, deep learning, and graph networks,” *arXiv preprint*, 2018.
- [6] R. Ying, R. He, K. Chen, P. Eksombatchai, W. L. Hamilton, and J. Leskovec, “Graph convolutional neural networks for web-scale recommender systems,” in *KDD*, 2018.
- [7] F. Monti, F. Frasca, D. Eynard, D. Mannion, and M. M. Bronstein, “Fake news detection on social media using geometric deep learning,” *arXiv preprint*, 2019.
- [8] J. M. Stokes, K. Yang, K. Swanson, W. Jin, A. Cubillos-Ruiz, N. M. Donghia, C. R. MacNair, S. French, L. A. Carfrae, Z. Bloom-Ackermann *et al.*, “A deep learning approach to antibiotic discovery,” *Cell*, 2020.
- [9] P. Gainza, F. Sverrisson, F. Monti, E. Rodola, D. Boscai, M. Bronstein, and B. Correia, “Deciphering interaction fingerprints from protein molecular surfaces using geometric deep learning,” *Nature Methods*, 2020.
- [10] Y. Long, M. Wu, C. K. Kwok, J. Luo, and X. Li, “Predicting human microbe–drug associations via graph convolutional network with conditional random field,” *Bioinformatics*, 2020.
- [11] W. Hu, M. Fey, M. Zitnik, Y. Dong, H. Ren, B. Liu, M. Catasta, and J. Leskovec, “Open graph benchmark: Datasets for machine learning on graphs,” *arXiv preprint*, 2020.
- [12] W. Hu, M. Fey, H. Ren, M. Nakata, Y. Dong, and J. Leskovec, “Ogb-lsc: A large-scale challenge for machine learning on graphs,” in *KDD Cup*, 2021.
- [13] R. Addanki, P. W. Battaglia, D. Budden, A. Deac, J. Godwin, T. Keck, W. L. S. Li, A. Sanchez-Gonzalez, J. Stott, S. Thakoor *et al.*, “Large-scale graph representation learning with very deep gnn and self-supervision,” in *KDD Cup*, 2021.
- [14] K. Xu, W. Hu, J. Leskovec, and S. Jegelka, “How powerful are graph neural networks?” in *ICLR*, 2019.
- [15] G. Li, M. Müller, A. Thabet, and B. Ghanem, “Deepgcn: Can gcn go as deep as cnn?” in *ICCV*, 2019.
- [16] G. Corso, L. Cavigliari, D. Beaini, P. Liò, and P. Veličković, “Principal neighbourhood aggregation for graph nets,” *NeurIPS*, 2020.
- [17] V. P. Dwivedi, C. K. Joshi, T. Laurent, Y. Bengio, and X. Bresson, “Benchmarking graph neural networks,” *arXiv preprint*, 2020.
- [18] W. Hu, B. Liu, J. Gomes, M. Zitnik, P. Liang, V. Pande, and J. Leskovec, “Strategies for pre-training graph neural networks,” in *ICLR*, 2019.
- [19] Y. You, T. Chen, Y. Sui, T. Chen, Z. Wang, and Y. Shen, “Graph contrastive learning with augmentations,” *NeurIPS*, 2020.
- [20] J. Qiu, Q. Chen, Y. Dong, J. Zhang, H. Yang, M. Ding, K. Wang, and J. Tang, “Gcc: Graph contrastive coding for graph neural network pre-training,” in *KDD*, 2020.
- [21] Y. Jiao, Y. Xiong, J. Zhang, Y. Zhang, T. Zhang, and Y. Zhu, “Sub-graph contrast for scalable self-supervised graph representation learning,” in *ICDM*, 2020.
- [22] F. Frasca, E. Rossi, D. Eynard, B. Chamberlain, M. Bronstein, and F. Monti, “Sign: Scalable inception graph neural networks,” in *ICML Workshop on Graph Representation Learning and Beyond*, 2020.
- [23] S. A. Tailor, F. L. Opolka, P. Liò, and N. D. Lane, “Adaptive filters and aggregator fusion for efficient graph convolutions,” in *MLSys GNNs Sys Workshop*, 2021.
- [24] G. Li, M. Müller, B. Ghanem, and V. Koltun, “Training graph neural networks with 1000 layers,” in *ICML*, 2021.
- [25] Y. Gao, H. Yang, P. Zhang, C. Zhou, and Y. Hu, “Graph neural architecture search,” in *IJCAI*, 2020.
- [26] Y. Zhao, D. Wang, X. Gao, R. Mullins, P. Liò, and M. Jamnik, “Probabilistic dual network architecture search on graphs,” in *AAAI Workshop*, 2021.
- [27] Y. Zhao, D. Wang, D. Bates, R. Mullins, M. Jamnik, and P. Liò, “Learned low precision graph neural networks,” *arXiv preprint*, 2020.
- [28] S. A. Tailor, J. Fernandez-Marques, and N. D. Lane, “Degree-quant: Quantization-aware training for graph neural networks,” in *ICLR*, 2021.
- [29] G. Hinton, O. Vinyals, and J. Dean, “Distilling the knowledge in a neural network,” *arXiv preprint*, 2015.
- [30] J. Gou, B. Yu, S. J. Maybank, and D. Tao, “Knowledge distillation: A survey,” *International Journal of Computer Vision*, 2021.
- [31] Y. Yang, J. Qiu, M. Song, D. Tao, and X. Wang, “Distilling knowledge from graph convolutional networks,” in *CVPR*, 2020.
- [32] A. Romero, N. Ballas, S. E. Kahou, A. Chassang, C. Gatta, and Y. Bengio, “Fitnets: Hints for thin deep nets,” *arXiv preprint*, 2014.
- [33] Q. Li, S. Jin, and J. Yan, “Mimicking very efficient network for object detection,” in *CVPR*, 2017.
- [34] G.-H. Wang, Y. Ge, and J. Wu, “In defense of feature mimicking for knowledge distillation,” *arXiv preprint*, 2020.
- [35] S. Zagoruyko and N. Komodakis, “Paying more attention to attention: Improving the performance of convolutional neural networks via attention transfer,” *arXiv preprint*, 2016.
- [36] A. Loukas, “What graph neural networks cannot learn: depth vs width,” in *ICLR*, 2020.
- [37] A. v. d. Oord, Y. Li, and O. Vinyals, “Representation learning with contrastive predictive coding,” *arXiv preprint*, 2018.
- [38] Z. Wu, Y. Xiong, S. X. Yu, and D. Lin, “Unsupervised feature learning via non-parametric instance discrimination,” in *CVPR*, 2018.
- [39] T. Chen, S. Kornblith, M. Norouzi, and G. Hinton, “A simple framework for contrastive learning of visual representations,” in *ICML*, 2020.
- [40] Y. Tian, D. Krishnan, and P. Isola, “Contrastive representation distillation,” in *ICLR*, 2019.

- [41] I. Armeni, O. Sener, A. R. Zamir, H. Jiang, I. Brilakis, M. Fischer, and S. Savarese, "3d semantic parsing of large-scale indoor spaces," in *CVPR*, 2016.
- [42] B. Yan, C. Wang, G. Guo, and Y. Lou, "Tinygnn: Learning efficient graph neural networks," in *KDD*, 2020.
- [43] C. K. Joshi, T. Laurent, and X. Bresson, "An efficient graph convolutional network technique for the travelling salesman problem," *arXiv preprint*, 2019.
- [44] Q. Cappart, D. Chételat, E. Khalil, A. Lodi, C. Morris, and P. Veličković, "Combinatorial optimization and reasoning with graph neural networks," in *IJCAI*, 2021.
- [45] Y. Liu, J. Cao, B. Li, C. Yuan, W. Hu, Y. Li, and Y. Duan, "Knowledge distillation via instance relationship graph," in *CVPR*, 2019.
- [46] W. Park, D. Kim, Y. Lu, and M. Cho, "Relational knowledge distillation," in *CVPR*, 2019.
- [47] F. Tung and G. Mori, "Similarity-preserving knowledge distillation," in *ICCV*, 2019.
- [48] W. Zhang, X. Miao, Y. Shao, J. Jiang, L. Chen, O. Ruas, and B. Cui, "Reliable data distillation on graph convolutional network," in *SIGMOD*, 2020.
- [49] C. Yang, J. Liu, and C. Shi, "Extract the knowledge of graph neural networks and go beyond it: An effective knowledge distillation framework," *arXiv preprint*, 2021.
- [50] Y. Chen, Y. Bian, X. Xiao, Y. Rong, T. Xu, and J. Huang, "On self-distilling graph neural network," *arXiv preprint*, 2020.
- [51] H. Zhang, S. Lin, W. Liu, P. Zhou, J. Tang, X. Liang, and E. P. Xing, "Iterative graph self-distillation," *arXiv preprint*, 2020.
- [52] X. Deng and Z. Zhang, "Graph-free knowledge distillation for graph neural networks," in *IJCAI*, 2021.
- [53] H. Stärk, D. Beaini, G. Corso, P. Tossou, C. Dallago, S. Günemann, and P. Liò, "3d infomax improves gnns for molecular property prediction," *arXiv preprint*, 2021.
- [54] S. Liu, H. Wang, W. Liu, J. Lasenby, H. Guo, and J. Tang, "Pre-training molecular graph representation with 3d geometry," *arXiv preprint*, 2021.
- [55] D. Mesquita, A. Souza, and S. Kaski, "Rethinking pooling in graph neural networks," in *NeurIPS*, 2020.
- [56] M. M. Bronstein, J. Bruna, T. Cohen, and P. Veličković, "Geometric deep learning: Grids, groups, graphs, geodesics, and gauges," *arXiv preprint*, 2021.
- [57] C. Joshi, "Transformers are graph neural networks," *The Gradient*, 2020.
- [58] C. R. Qi, L. Yi, H. Su, and L. J. Guibas, "Pointnet++: Deep hierarchical feature learning on point sets in a metric space," in *NIPS*, 2017.
- [59] H. Thomas, C. R. Qi, J.-E. Deschaut, B. Marcotegui, F. Goulette, and L. J. Guibas, "Kpconv: Flexible and deformable convolution for point clouds," *CVPR*, 2019.
- [60] C. Choy, J. Gwak, and S. Savarese, "4d spatio-temporal convnets: Minkowski convolutional neural networks," in *CVPR*, 2019.
- [61] Z. Liu, H. Tang, Y. Lin, and S. Han, "Point-voxel cnn for efficient 3d deep learning," in *NeurIPS*, 2019.
- [62] H. Tang, Z. Liu, S. Zhao, Y. Lin, J. Lin, H. Wang, and S. Han, "Searching efficient 3d architectures with sparse point-voxel convolution," in *ECCV*, 2020.
- [63] T. Chaton, C. Nicolas, S. Horache, and L. Landrieu, "Torch-points3d: A modular multi-task framework for reproducible deep learning on 3d point clouds," in *3DV*, 2020.
- [64] Z. Wu, B. Ramsundar, E. N. Feinberg, J. Gomes, C. Geniesse, A. S. Pappu, K. Leswing, and V. Pande, "Moleculenet: a benchmark for molecular machine learning," *Chemical science*, 2018.
- [65] K. Wang, I. Shen, C. Huang, C.-H. Wu, Y. Dong, and A. Kanakia, "Microsoft academic graph: when experts are not enough," *Quantitative Science Studies*, 2020.
- [66] Z. Wu, S. Song, A. Khosla, F. Yu, L. Zhang, X. Tang, and J. Xiao, "3d shapenets: A deep representation for volumetric shapes," in *CVPR*, 2015.
- [67] M. A. Uy, Q.-H. Pham, B.-S. Hua, D. T. Nguyen, and S.-K. Yeung, "Revisiting point cloud classification: A new benchmark dataset and classification model on real-world data," in *ICCV*, 2019.
- [68] M. Schlichtkrull, T. N. Kipf, P. Bloem, R. Van Den Berg, I. Titov, and M. Welling, "Modeling relational data with graph convolutional networks," in *European semantic web conference*, 2018.
- [69] M. Fey and J. E. Lenssen, "Fast graph representation learning with pytorch geometric," *arXiv preprint*, 2019.
- [70] A. Al Badawi, J. Chao, J. Lin, C. F. Mun, S. J. Jie, B. H. M. Tan, X. Nan, A. M. M. Khin, and V. Chandrasekhar, "Towards the alexnet moment for homomorphic encryption: Hcnn, the first homomorphic cnn on encrypted data with gpus," *IEEE Transactions on Emerging Topics in Computing*, 2020.
- [71] S. Kornblith, M. Norouzi, H. Lee, and G. Hinton, "Similarity of neural network representations revisited," in *ICML*, 2019.
- [72] N. Mantel, "The detection of disease clustering and a generalized regression approach," *Cancer research*, 1967.
- [73] H. Zeng, H. Zhou, A. Srivastava, R. Kannan, and V. Prasanna, "Graph-saint: Graph sampling based inductive learning method," in *ICLR*, 2020.
- [74] Q. Huang, H. He, A. Singh, S.-N. Lim, and A. Benson, "Combining label propagation and simple models out-performs graph neural networks," in *ICLR*, 2021.
- [75] T. Nguyen, M. Raghu, and S. Kornblith, "Do wide and deep networks learn the same things? uncovering how neural network representations vary with width and depth," in *ICLR*, 2021.
- [76] P. Legendre and L. Legendre, *Numerical ecology*. Elsevier, 2012.

## APPENDIX

### A. Additional Results

In Tab.X, we attempt to reproduce the results from Yang et. al. [31], but our codebase<sup>4</sup> showed significant improvements over their numbers for the same teacher-student pair. We found negligible performance difference between the two models, even under supervised learning. Thus, we redo the experiment with a more reasonable student architecture (a 2 layer GAT instead of 5 layers) and find that G-CRD leads to the best performance, followed by LSP. We believe small-scale and saturated datasets such as PPI or ModelNet with random splits are not suitable for benchmarking distillation techniques. We advocate for the use of large-scale datasets with realistic data splits which evaluate out-of-distribution generalization.

TABLE X: **Node classification on PPI** (metric: F1 (%)). We report the average performance and std. across 10 random seeds.

Teacher (#Layer,#Param):		GAT (3L,3.6M)	GAT (3L,3.6M)
Student (#Layer,#Param):		GAT (5L,160K)	GAT (2L,180K)
		Reported	Our Codebase
Sup.	Supervised Teacher	97.6	97.95 ±0.10
	Supervised Student	95.7	97.90 ±0.45
Distillation	KD [29]	-	97.93 ±0.26
	FitNet [32]	95.6	97.74 ±0.34 (↓)
	AT [35]	95.4	97.02 ±0.76 (↓)
	LSP [31]	96.1	97.81 ±0.31 (↓)
	GNN-SD [50]	96.2	-
	G-CRD (Ours)	-	98.42 ±0.14 (↑)

In Tab.XI, we show additional results on MOLHIV when combining KD with representation distillation. The combination of G-CRD with KD leads to the best performance.

TABLE XI: **Molecular graph classification on MOLHIV** (metric: ROC-AUC (%)). Additional results for combining KD with representation distillation techniques.

Teacher (#Layer,#Param):		PNA (5L,2.4M)	PNA (5L,2.4M)
Student (#Layer,#Param):		GCN (2L,15K)	GCN (2L,40K)
Sup.	Supervised Teacher	77.48 ±1.71	77.48 ±1.71
	Supervised Student	73.02 ±1.46	73.65 ±1.50
Distillation	KD [29]	74.13 ±1.72	74.45 ±1.27
	KD + FitNet [32]	73.77 ±1.20 (↓)	74.16 ±1.90 (↓)
	KD + AT [35]	73.42 ±1.67 (↓)	75.22 ±1.61 (↑)
	KD + LSP [31]	74.18 ±1.47 (↑)	75.08 ±1.43 (↑)
	KD + GSP (Ours)	74.19 ±1.41 (↑)	74.87 ±1.19 (↑)
	KD + G-CRD (Ours)	74.74 ±1.59 (↑)	76.26 ±0.79 (↑)

<sup>4</sup>We built our implementation upon the official PyG example for PPI.

## B. Pseudocode

Listings 1 and 2, provide PyTorch-style pseudocode for the GSP and G-CRD representation distillation objectives, respectively.

```

1 import torch
2 import torch.nn.functional as F
3
4 def gsp_cosine_criterion(
5     student_feat, # features from student model
6     teacher_feat, # features from teacher model
7 ):
8
9     # L2-normalize student features
10    # dim: (n, d_s)
11    student_feat = F.normalize(
12        student_feat, p=2, dim=-1
13    )
14
15    # L2-normalize teacher features
16    # dim: (n, d_t)
17    teacher_feat = F.normalize(
18        teacher_feat, p=2, dim=-1
19    )
20
21    # all pairwise cosine similarities for student
22    # dim: (n, d_s).(d_s, n) -> (n, n)
23    student_pw_sim = torch.mm(
24        student_feat, student_feat.transpose(0, 1)
25    )
26
27    # all pairwise cosine similarities for teacher
28    # dim: (n, d_t).(d_t, n) -> (n, n)
29    teacher_pw_sim = torch.mm(
30        teacher_feat, teacher_feat.transpose(0, 1)
31    )
32
33    # regression to match pairwise similarities
34    loss_gsp = F.mse_loss(
35        student_pw_sim, teacher_pw_sim
36    )
37
38    return loss_gsp

```

Listing 1: PyTorch-style pseudocode for the Global Structure Preserving objective with cosine pairwise similarity kernel.

```

1 import torch
2 import torch.nn.functional as F
3
4 def gcrd_criterion(
5     student_feat, # features from student model
6     teacher_feat, # features from teacher model
7     student_proj_head, # learnt projection head
8     teacher_proj_head, # learnt projection head
9     nce_tau # InfoNCE temperature
10 ):
11
12    # project and L2-normalize student features
13    # dim: (n, d_s) -> (n, d)
14    student_feat = F.normalize(
15        student_proj_head(student_feat),
16        p=2, dim=-1
17    )
18
19    # project and L2-normalize teacher features
20    # dim: (n, d_t) -> (n, d)
21    teacher_feat = F.normalize(
22        teacher_proj_head(teacher_feat),
23        p=2, dim=-1
24    )
25
26    # cosine similarities b/w student and teacher
27    # dim: (n, d).(d, n) -> (n, n)
28    nce_logits = torch.mm(
29        student_feat, teacher_feat.transpose(0, 1)
30    )
31
32    # prepare labels for correspondence task
33    # dim: (n, 1)
34    nce_labels = torch.arange(student_feat.shape[0])
35
36    # temperature-scaled softmax cross entropy
37    loss_nce = F.cross_entropy(
38        nce_logits/ nce_tau, nce_labels
39    )
40
41    return loss_nce

```

Listing 2: PyTorch-style pseudocode for the Graph Contrastive Representation Distillation objective.